Physica Medica 57 (2019) 245–250

Contents lists available at ScienceDirect

Physica Medica

journal homepage: www.elsevier.com/locate/ejmp

Original paper

Pre and post operative radiation protection in Ru-106 brachytherapy ophthalmic plaque surgery and related material shielding properties

Simone Busoni[a,*], Luca Fedeli[b], Giacomo Belli[a], Elisabetta Genovese[c], Vittorio Cannatà[c], Cesare Gori[b], Francesco Rossi[a]

[a] A.O.U. Careggi, Firenze, Italy
[b] Università degli Studi di Firenze, Firenze, Italy
[c] Ospedale Pediatrico Bambino Gesù, Roma, Italy

ARTICLE INFO

Keywords:
^{106}Ru brachytherapy
^{106}Ru radiation protection
^{106}Ru attenuation materials properties

ABSTRACT

Pre and post-operative exposure levels of medical staff and people from public in intra-operative Ru-106 ophthalmic brachytherapy are reported, together with attenuation properties of selected shielding materials. In particular radiation exposure of workers during plaque transportation and during medical assistance of implanted plaque patient was measured. Taking into account dose rates and considering standard assistance procedure of hospitalized patients, the exposure of medical staff and people of the public were evaluated for a given workload.

In order to provide tools to optimize radiation protection, considering social and economic aspects due to possible hospital discharge or hospital stay, the attenuation properties of common shielding materials (lead, concrete, red brick, PMMA and gypsum) were measured, considering both narrow and broad beam setups. The eye was simulated using a water equivalent phantom and plaque was fixed on it. All measurements were performed with calibrated survey meters. Results were compared with numerical simulation of bremsstrahlung X-ray radiation spectra emitted from patient eye.

Exposure levels measured at 1 m distance in front of the implanted eye are 0.05 μSv/h/MBq, at 10 cm from patient head, 0.44 μSv/h/MBq (plaque side), 0.4 μSv/h/MBq (front), 0.25 μSv/h/MBq (lateral, opposed to plaque), 0.2 μSv/h/MBq (back).

Average exposure levels, under conservative assumptions, for medical staff is 17 μSv/patient and less than 23 μSv/patient for careers and comforters. TVLs in lead and concrete are about 1.6 cm and 11.5 cm respectively.

1. Introduction

The use of ^{106}Ru/^{106}Rh (^{106}Ru in the following) plaque was introduced in 1964 for choroidal melanomas therapy [1] nowadays is adopted in both LDR and HDR brachytherapy [2–6]. The radioisotope emits β radiation with an end-point energy of 3.5 MeV [7] and X-γ rays of energy between 0.5 and 1.6 MeV [8]. The plaque is like a stainless steel contact lens, with lateral holes for the surgical implantation. On the convex part of the plaque a thin layer of the isotope is deposed.

Considered technique is based on the surgical implantation of the plaque directly on the eye of the patient, on the side where the treatment is needed. Plaque remains implanted and is surgically removed after a therapeutic suitable time, defined by medical staff in advance, (usually few days). Patient may undergo clinical recovery or may be dismissed during the implantation period, depending on clinical conditions and local hospital protocols.

While data of surgeon exposure during surgery and patient dose are available [9,10] there is lack of data with respect to exposure rates of workers and people from public in pre and post-operative phase.

The aim the of present study is to consider, in a typical clinical scenario, occupational workers and public exposure levels and to evaluate shielding properties of commonly used materials. Data are required in order to optimize radiation protection, considering social and economic aspects due to possible patient hospital discharge or recovery, and to guarantee not to exceed exposure limits of workers and public (ICRP [11], IAEA BSS [12] and COUNCIL DIRECTIVE 2013/59/EURATOM [13]).

Exposure levels close to implanted patients and close to container were evaluated for caregivers and medical staff, in particular the dose to nurses involved in surgical rooms or in patient care during the

* Corresponding author.
E-mail addresses: busonis@aou-careggi.toscana.it (S. Busoni), luca.fedeli@unifi.it (L. Fedeli).

https://doi.org/10.1016/j.ejmp.2018.11.003
Received 16 July 2018; Received in revised form 3 October 2018; Accepted 5 November 2018
Available online 18 December 2018

clinical recovery, paramedical dedicated to plaque transportation and other professionals close to the patient during the recovery.

Moreover, laboratory measurements were performed on selected materials to evaluate their attenuation properties and build-up factors. Numerical simulation of X-γ and Bremsstrahlung (BS) spectrum, generated from beta radiation of ^{106}Ru in eye, was performed and results are compared both with in vivo and laboratory measurements.

Maximum number of treated patients not to exceed public exposure limits is provided, considering typical plaque activity and reasonable recovery procedure.

2. Materials and methods

^{106}Ru plaques are spherically shaped, with the inner radius of curvature ranging from 12 mm to 14 mm, and their diameter varying between 11.6 mm and 25.4 mm, different shapes are available, depending from specific clinical therapy. The active material is deposited on a 0.7 mm pure silver bulk and covered with 0.1 mm of pure silver. Plaque nominal activity varies between 5 MBq and 50 MBq. Shipping box is a Type A package, UN 2910 (according to international ADR protocol) with transportation index of 0.1. As for intra-hospital transportation a dedicated shielding cylindrical multilayer steel box, that may be used for plaque sterilisation, is provided by manufacturer. In Fig. 1 a sketch of the considered plaque is shown.

In order to optimize radiation protection, two different workers exposure conditions were considered: during plaque transportation and close to patient with implanted plaque. Numerical simulation of dose rate from BS and x-γ radiation was also performed and compared with measurements around patient with implanted plaque.

Characterization of radiation shielding properties of BS and x-γ radiation was performed considering several common attenuation layers and experimental results were compared with numerical simulation.

2.1. Occupational and public exposure in pre and post surgery phase

In vivo measurements were performed on nine implanted patients. Five different positions around patient head were considered. In particular *Plaque side* refers to the side of the head closest to eye with implanted plaque, *Front* is in front of the eye with the plaque, *Contralateral* is opposed to *Plaque side*, *Nape* is opposed to *Front*, and *Top* is above the head, distances from patient skin were of 10 and 50 cm. Nominal plaque activity varied from 6.8 and 36 MBq, dose rates were normalized to plaque activity. All measurements were performed with a calibrated ionization chamber (Victoreen 451, Fluke Corp.,WA, USA).

Intra-hospital plaque transportation is performed employing the manufacturer package, that is a multi-layer cylindrical box (external diameter and height of 10 cm). Inner layer is made of a plastic container (3.5 cm diameter and height); a second layer is made of aluminium (5 mm thick). The external layer is made of stainless steel (10 mm thick)

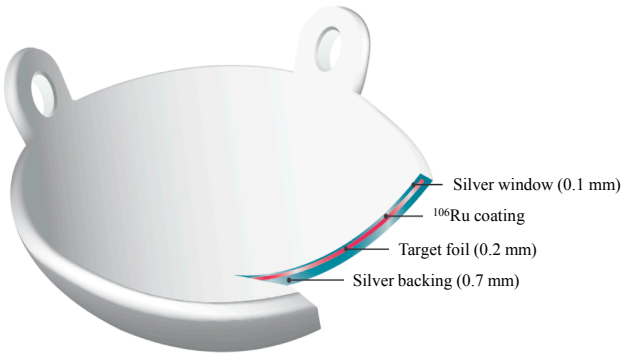

Fig. 1. Scheme of ^{106}Ru plaques.

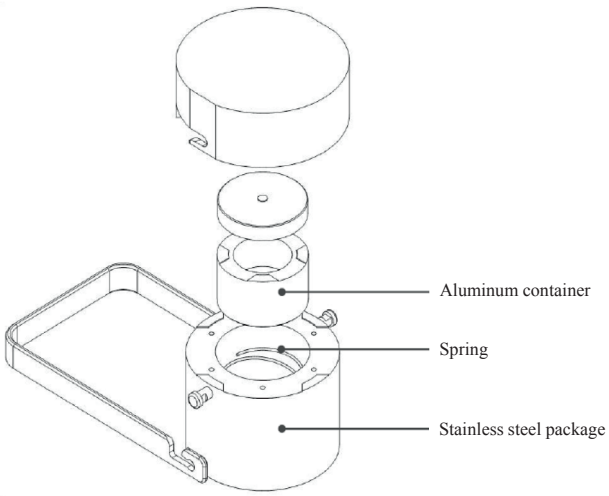

Fig. 2. Scheme of ^{106}Ru plaque transportation package.

and contains a special holder (spring) to avoid aluminium container movements. In addition, the box comes with a removable handle that blocks the cap, preventing from accidentally opening the container; in Fig. 2 a schematic representation of package is reported.

Manufacturer recommends to put eye plaque into the aluminium container with the concave side (radiation window) facing downward to reduce radiation exposure.

Radiation dose rate measurements around transportation package were performed considering different plaque orientation inside the container. Dose rate measurement were performed with a dose rate detector (Automesse SZINTOMAT 6134); before the measurement, detector response was verified using an high-activity (20 MBq) ^{90}Sr beta calibration source. Dose rate was measured considering a plaque with nominal activity of 6.8 MBq, and a distance up to 100 cm in several directions (side and top).

A custom code (developed with Mathematica 9.0, Wolfram Champaign, IL USA) was written to perform numerical simulation of the BS spectrum; beta energy spectrum of ^{106}Ru was taken from [1]. Photon BS spectrum generated from eye (considered as a 25 mm diameter sphere) was calculated. BS appropriate cross-section was considered [14] and electron continuous slowing down approximation (CSDA) was used; spectrum normalization was performed using radiation yield tables [15].

The exposure rates were estimated using the Flux-to-Dose-Rate conversion function [16] and attenuation of selected materials (lead and concrete) was calculated.

Considering a monochromatic electron with kinetic energy T_0, passing through some material and emitting X-ray BS, the emitted photons spectrum, was:

$$\frac{dn}{dk} = \frac{N_a}{A} r_{eff} \rho \frac{d\sigma_k}{dk}(k, T_0) \tag{1}$$

where N_α is number of Avogadro, A is the atomic mass of the medium crossed, r_{eff} is the effective range of the electron in the medium, ρ is the material density and $\frac{d\sigma_k}{dk}(k, T_0)$ is the Bremsstrahlung cross-section. Considering CSDA, the value of r_{eff} can be determinate from the radiation yield y_e (listed in [15]):

$$r_{eff} = \frac{T_0 y_e}{\int_0^{T_0} k \frac{d\sigma_k}{dk}(k, T_0) dk} \frac{A}{N_a} \tag{2}$$

Considering a continuum electron spectrum, BS X-ray emission was calculated as

$$\frac{dn_{BS}}{dk} = \int_k^{E_M} \frac{dn}{dk}(k, T_0) \beta(T_0) dT_0 \tag{3}$$

E_M is the end-point energy of the beta spectrum and $\beta(T_0)$ is the probability distribution function of beta spectrum (i.e. $\int_0^{E_M} \beta(x)dx = 1$).

Full spectrum was calculated considering both the BS and X-gamma radiation of ^{106}Ru contribution. Eye attenuation was considered in order to determinate the correct dose rate, in particular BS spectrum was highly filtered from eye itself.

Full spectrum is:

$$\frac{dn_{eye}}{dk} = \frac{dn_{BS}}{dk} e^{-\mu(k)d_e} + \sum_i BR_i e^{-\mu(k_i)d_e}\delta(k - k_i) \quad (4)$$

where $\mu(k)$ is the attenuation coefficient of the eye (considered as water) relative to photon energy k, listed in [15], d_ε is the diameter of the eye (25 mm), BR_i is the branching ratio of the i-th X-ray (or gamma-ray) emitted from ^{106}Ru (and k_i its energy) [8], δ is the Dirac-δ. In radiation protection, dose rate is considered, rather than photon flux, conversion was performed using Flux-to-Dose-Rate conversion function $f(k)$ [16]. The dose rate after layer attenuation of thickness x, was

$$\Gamma_{eye}(d) = \frac{1}{4\pi}\frac{S_{ref}}{d^2}\int_0^{E_M} \frac{dn_{eye}}{dk} f(k)dk \quad (5)$$

where S_{ref} is the reference surface (1 cm^2) and $\Gamma_{eye}(d)$ is the dose rate (in Hp(10)) at distance d from eye along the plaque-eye direction.

2.2. Materials attenuation properties

Material shielding properties were measured following IEC 61331-1:2014 [17] protocol, in particular both narrow and broad beam mode were considered. HVL and TVL were measured for five selected materials (lead (Pb), concrete, red brick, PMMA and gypsum). Measurements were performed simulating the eye with a 25 mm diameter plastic sphere, filled with water and the plaque attached on it. The plaque had an activity of 35.15 MBq. Detection limit (DL) were evaluated according to [18], using a truncated Gaussian distribution and considering the uncertainties propagation as described in [19] with 95% of confidence level (CL); only measurements above DL were considered. In Fig. 3 the experimental setup used for attenuation measurements is outlined. HVLs and TVLs were calculated considering mono exponential attenuation law and, for lead and concrete, results were compared with numerical simulation. Build up factors are reported.

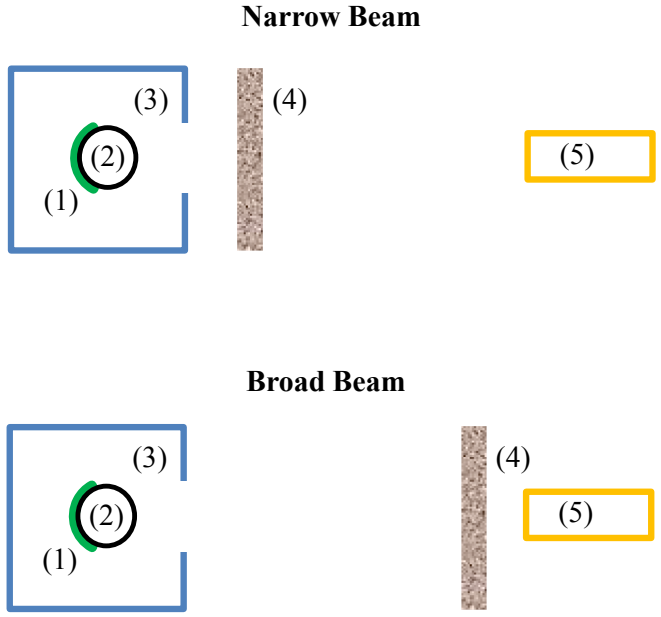

Fig. 3. Experimental setup for attenuation measurement (not in scale): (1) plaque, (2) eye phantom, (3) lead diaphragms, (4) attenuation layer, (5) detector.

Measurements were performed with a calibrated ionization chamber (Victoreen 451, Fluke Corp., WA, USA) and a portable spectrometer (IdentiFINDER-2, Flir Systems Inc., OR, USA) equipped with a 35 mm diameter × 51 mm length NaI (Tl) detector.

Using the same formalism as in previous section, dose rate after layer attenuation of thickness x, can be determinated:

$$\Gamma(d, x) = \frac{1}{4\pi}\frac{S_{ref}}{d^2}\int_0^{E_M} \frac{dn_{eye}}{dk} e^{-\mu_{mat}(k)x} f(k)dk \quad (6)$$

where S_{ref} is the reference surface (1 cm^2), μ_{mat} is the attenuation coefficient of attenuation layer[15] and $\Gamma(d, x)$ is the dose rate (in Hp (10)) at distance d from radiation source and attenuated from a thickness x of material.

Considering above formalism, half vale layer (HVL) and tenth vale layer (TVL) were calculated as (the choice of d is arbitrary):

$$\Gamma(d, HVL) = \frac{1}{2}\Gamma(d, 0); \qquad \Gamma(d, 0) = \frac{1}{10}\Gamma(d, 0) \quad (7)$$

3. Results

The average exposure levels (± SD) were measured around nine patients head are reported in Table 1; values are normalized to unit activity (μSv/h/MBq). Five positions around the head, at 10 cm distance from the skin, are considered, plus two positions at 1 m. *Plaque side* refers to the side of the head closest to eye with implanted plaque, *Front* is in front of the eye with the plaque, *Contralateral* is opposed to *Plaque side*, *Nape* is opposed to *Front*, and *Top* is above the head.

Table 2 shows the exposure levels measured around the different containers, both plastic and transportation package. These levels are nearly constant for any given direction and plaque orientation inside plastic package. During transportation, worker hands are about 10 cm away from stainless steel container, and considering a typical plaque activity of 25 MBq, exposure rate was 15 μSv/h.

In Table 3 numerical simulation of dose rate in Hp(10), normalised to 1 MBq plaque activity and at a reference distance of 1 m from patient, considering both BS generated from eye and ^{106}Ru X-γ rays is reported. Attenuation, considering two thicknesses of typical shielding materials (0.2 cm lead and 10 cm concrete), is also included. The *Eye Front* column refers to the dose rate calculated with the attenuation of the eye alone; *Pb* and *Concrete* refer to the dose rates after the attenuation of the eye and a shielding of 0.2 cm of lead and 10 cm of concrete respectively. First row shows dose rates from BS only, second row shows dose rates from X-γ radiation, the last one represents total dose rate (sum of the previous two rows).

Transmission measurements, in narrow and broad beam condition and as a function of attenuation layer thickness, were fitted using a mono exponential function ($R^2 > 0.95$ for all considered materials (concrete, red brick, lead, PMMA and gypsum)).

HVLs and TVLs are reported in Table 4, for the five considered attenuation materials; lead and concrete attenuation properties are compared with numerical simulation, showing good agreement within experimental uncertain.

In particular in Fig. 4 exposure rate transmission (measurements: blue points, simulated data: solid blue line) as a function of the attenuation layer thickness for lead is reported. In Fig. 5 exposure rate transmissions (measured results, red points and simulated data, dashed red line), considering concrete, was reported. Error bars are one SD in both figures.

Considering measurements uncertainties, transmission DL is 0.09, consequently values below this threshold are not statistically different from the background at a CL of 95%.

Build up factor are reported in Table 5, considering different materials and thickness. Build up factors range between 1.2 and 1.4 at one

Table 1
Normalized exposure levels around patient head (μSv/h/MBq).

Skin distance	Plaque side	Front	Contralateral	Nape	Top
10 cm	0.44 ± 0.08	0.40 ± 0.07	0.25 ± 0.04	0.20 ± 0.05	0.18 ± 0.04
1 m	0.05 ± 0.02	0.03 ± 0.01	–	–	–

Table 2
Normalized transportation exposure levels (μSv/h/MBq).

Distance	Plastic package	Transportation package
Contact	338 ± 34	5.9 ± 0.6
10 cm	29 ± 3	0.6 ± 0.1
50 cm	1.5 ± 0.1	0.13 ± 0.01

Table 3
Dose rate in Hp(10) at 1 m from radiation source (simulated results).

$H_p(10)$ (nSv/h/MBq)	Eye Front	Pb (0.2 cm)	Concrete (10 cm)
Bremsstrahlung	1.3	0.7	0.2
X-γ ray	26.2	19.2	3.9
Total	27.5	19.9	4.1

Table 4
Materials attenuation properties (narrow beam).

	Pb	Concrete	Red Brick	PMMA	Gypsum
HVL (cm)	0.4 ± 0.1	2.9 ± 0.4	5.1 ± 0.4	6.5 ± 0.6	12 ± 1.5
TVL (cm)	1.6 ± 0.2	11.5 ± 0.6	13.8 ± 0.8	21.6 ± 1.5	37.3 ± 2.2

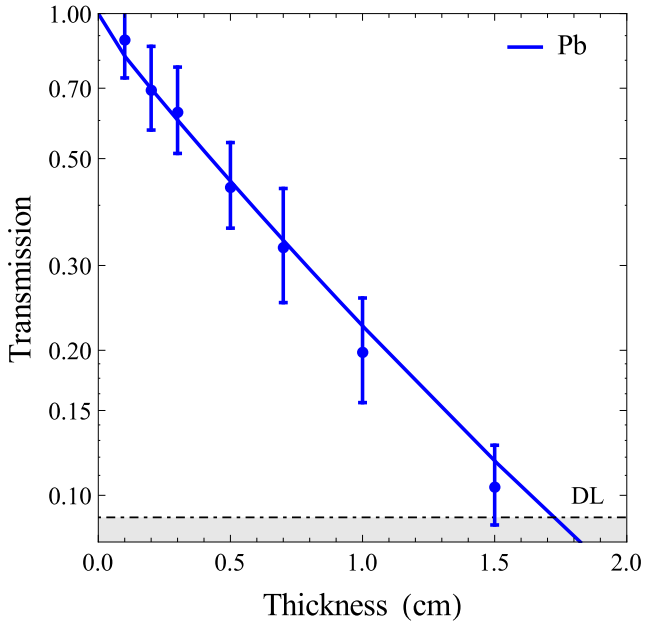

Fig. 4. Exposure rate transmission (measurements: blue points, simulated data: solid blue line) as a function of the attenuation layer thickness for lead. Error bars are one SD; Detection Limit (DL) is 0.9 (dashed-dotted black line). (For interpretation of the references to colour in this figure legend, the reader is referred to the web version of this article.)

HVL thickness, and between 2.1 and 2.8 at one TVL material thickness.

Simulated eye attenuated ^{106}Ru spectrum is reported in Fig. 6 (solid blue line), considering both contributions from BS and X-gamma ray. Attenuation considering two thicknesses of typical shielding materials (0.2 cm lead, dashed red line, and 10 cm concrete, dotted-dashed green)

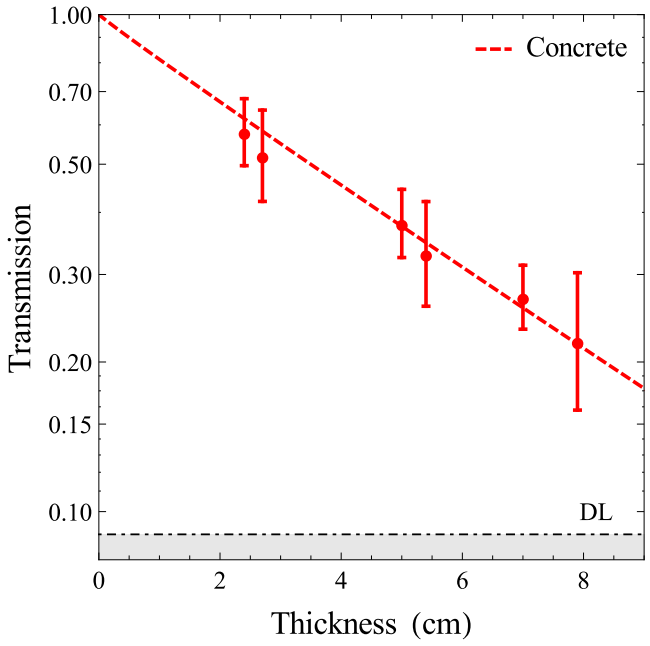

Fig. 5. Exposure rate transmission (measurements: red points, simulated data: dashed red line) as a function of the attenuation layer thickness for concrete. Error bars are one SD; Detection Limit (DL) is 0.9 (dashed-dotted black line). (For interpretation of the references to colour in this figure legend, the reader is referred to the web version of this article.)

Table 5
BUILD-UP FACTORS.

Thickness	Concrete	Red Brick	PMMA	Gypsum
HVL	1.4 ± 0.1	1.2 ± 0.1	1.3 ± 0.1	1.3 ± 0.1
TVL	2.8 ± 0.3	2.1 ± 0.2	2.2 ± 0.3	2.6 ± 0.2

is also included. The deep hollow around 90 keV in the lead attenuated spectrum is due to K-shell absorption. Larger contribution to total dose rate derives from X-γ rays, rather than from BS radiation.

4. Discussion

BS radiation represents a well know radioprotection issue when dealing with beta emitting radionuclides. In this study, both experimental measurements and simulations, taking into account BS radiation generated by ^{106}Ru in water, were performed and results were compared.

Considering a 25 MBq plaque activity, measurements at 10 cm apart from skin surface of the head of patient show a dose rate of the order of 11 μSv/h in front and on the plaque side; dose rates lower than 6.5 μSv/h were measured in other position around patient. One meter distance dose rate is below to 0.8 μSv/h.

Considering a 25 MBq plaque activity, measurements around transportation container indicate a 15 μSv/h dose rate emission at 10 cm and 3.3 μSv/h at 50 cm. Typical transportation time varies between a few minutes to half hour for each patient.

With the plaque in clinical use (i.e. implanted on the eye) the

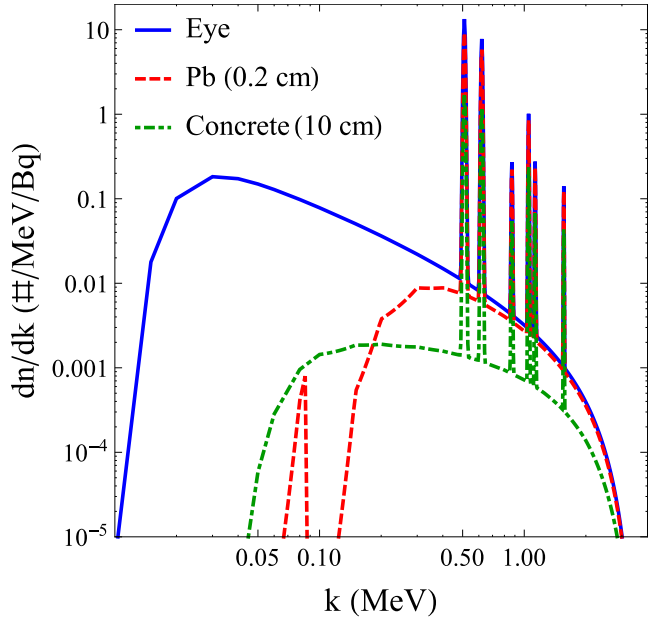

Fig. 6. Simulated results of ^{106}Ru full spectra, including the X-γ and the Bremsstrahlung radiation generated from the eye (solid blue line). Attenuation considering two thicknesses of typical shielding materials (0.2 cm lead, dashed red line, and 10 cm concrete, dotted-dashed green) is also included. (For interpretation of the references to colour in this figure legend, the reader is referred to the web version of this article.)

dominant contribution to dose rate derives from high-energy X-γ radiation (between 0.5 MeV and 1.6 MeV), BS contribution to total dose rate is lower than 5%. Simulated dose rate and in vivo measurement difference is the order of 10%.

4.1. Occupational and public exposure in pre and post surgery phase

In the following, a reasonable clinical scenario is considered and a plaque activity of 25 MBq is assumed.

Considering a worker (e.g. nurse) who assists hospitalized patients three times in a day, for 10 min for each operation, standing at 30 cm apart from patient, and a recovery time of three days for each implant, the effective dose is around 17 μSv/pt. Required not to exceed an annual exposure limit of 1 mSv/y effective dose, a single worker is allowed to assist around 60 patients.

In the same hypothesis, the annual dose for people standing at 1.5 m from a patient, for 8 h in a day (e.g. worker in an office next to patient room, neglecting the wall shielding), considering 60 patients in a year, each one hospitalized for three days, is around 0.65 mSv/y. For people of the public, considering a conservative total amount of 24 h spent around the patient at 1 m, during three implanted days, total exposure is around 23 μSv.

Dose rate at 50 cm from transportation container is about 3.3 μSv/h. Assuming a total transportation time of half hour for each patient, and a total of 60 patients in a year, the total dose of a worker who transport the plaque is less than 100 μSv/y (considering a conservative distance from the plaque of 50 cm during all transportation time).

4.2. Materials attenuation properties

In order to provide the reader a tool to calculate the required shielding thickness under different conditions, shielding properties were evaluated for five commonly used materials: lead, concrete, red brick, PMMA and gypsum. According to international standards (IEC 61331-1) both narrow and broad beam attenuation measurement were considered: HVLs, TVLs and build-up factors were calculated. In particular lead TVL is 1.6 cm, concrete and red brick TVL are of the order 10 cm, larger values were obtained for PMMA (22 cm) and gypsum (37 cm).

Build-up factors were calculated for the above considered five materials, values ranging between 1.2 and 1.4 considering one HVL thickness, and between 2.1 and 2.8 at one TVL thickness; results are in agreement with data found in literature for concrete [20]. Lead and concrete narrow beam laboratory measurements are in agreement with numerical simulation within 10%. Proposed BS spectrum simulation may be extended to different materials and beta sources.

5. Conclusions

In this study in vivo exposure measurements around patient with ^{106}Ru implanted plaque were performed. Considering a conservative clinical setup (i.e. large recovery and assistance times), a single worker assisting all annual hospitalized patients and a typical activity of the implanted plaques of 25 MBq, up to 60 patients may be treated in a year, without exceeding dose threshold of 1 mSv/y.

For the same number of patients, considering a person who works in office next to recovery room (i.e. a 8 h/day standing at 1.5 m from the patient bed), the received dose was around 0.65 mSv/y.

In the before mentioned scenario, received effective dose during plaque transportation was lower than 100 μSv/y and hand dose lower than 0.5 mSv.

As for exposure of the public (e.g. patient relatives, standing three days at 1 m from plaque implanted eye) it is not relevant from a radiation protection point of view (i.e. lower than 30 μSv).

Agreement between laboratory measurements and numerical simulation of ^{106}Ru BS spectrum generated from beta particles in plaque implanted eye was found. Larger contribution to radiation dose rate was from X-γ ray, BS contribution to total radiation is below 5% in all considered scenarios.

In synthesis, the use of ^{106}Ru plaque for ophthalmic treatments, considering a workload up to about 60 patients/year and the afore mentioned exposure time assumptions, does not require specific radiation protection shielding or dose reduction procedures in pre and post-operative phases, for both medical staff and people from public.

Acknowledgments

This research did not receive any specific grant from funding agencies in the public, commercial, or not-for-profit sectors.

References

[1] Lommatzsch P, Vollmar R. A new way in the conservative therapy of intraocular tumors by means of beta-irradiation (Ruthenium 106) with preservation of vision. Klin Monbl Augenheilkd 1966;148(5):682–99. German. PubMed PMID: 5996539.
[2] Genovese E, et al. Verification of dose distribution from CCX RU-106 eye-plaques by using a microDiamond dosimeter. Physica Medica: Eur J Med Phys 2016;32:26–7.
[3] Malone Ciaran, et al. Investigation of EBT3 film and the new PTW Microdiamond detector in verifying Ru-106 eye plaque dose calibrations. Physica Medica: Eur J Med Phys 2016;32(2):427.
[4] Espensen C, Fog L, Thariat J, Herault J, Aznar M, Maschi C, et al. Comparative dose planning for Ru-106 brachytherapy and proton therapy for choroidal melanomas. Physica Med 2018;52:1–98.
[5] Mostafa L, Rachid K, Ahmed SM. Comparison between beta radiation dose distribution due to LDR and HDR ocular brachytherapy applicators using GATE Monte Carlo platform. Phys Med 2016;32(8):1007–18.
[6] Quast U, Kaulich TW, Álvarez-Romero JT, Tedgren ÅC, Enger SA, Medich DC, et al. Perez-Calatayud, and others. A brachytherapy photon radiation quality index QBT for probe-type dosimetry. Phys Med 2016;32(6):741–8.
[7] Browne E, Firestone RB. Table of Radioactive Isotopes. Wiley-Interscience; 1986.
[8] Nucléide – Lara - Library for gamma and alpha emissions, http://www.nucleide.org/Laraweb.
[9] Laube Thomas, Fluhs Dirk, Kessler Cecilia, Bornfeld Norbert. Ophthalmology – determination of Surgeon's Absorbed Dose in Iodine 125 and Ruthenium 106. Ophthalmic Plaque Surgery 1999;2000(107):366–9.
[10] Sánchez-Reyes AI, Tello JI, Guix B, Salvat F. Monte Carlo calculation of the dose distributions of two 106Ru eye applicators. Radiother Oncol 1998

Nov;49(2):191–6.
[11] International Commission on Radiological Protection. The 2007 Recommendations of the International Commission on Radiological Protection. ICRP publication 103. Ann ICRP, 2007, 37, 1–332.
[12] IAEA Safety Standards Series No. GSR Part 3; ISBN:978-92-0-135310-8.
[13] COUNCIL DIRECTIVE 2013/59/EURATOM of 5 December 2013 laying down basic safety standards for protection against the dangers arising from exposure to ionising radiation, and repealing Directives 89/618/Euratom, 90/641/Euratom, 96/29/Euratom, 97/43/Euratom and 2003/122/Euratom.
[14] Koch HW, Motz JW. Reviews of Modern Physics, Bremsstrahlung Cross-Section Formulas and Related Data. Rev Mod Phys 1959;31(4).
[15] J. H. Hubbell, S. M. Seltzer, X-Ray Mass Attenuation Coefficients, https://www.nist.gov/pml/x-ray-mass-attenuation-coefficients.
[16] Kwon Seog-Guen, Kim Kyung-Eung, Ha Chung-Woo, Moon Philip S, Yook Chong-Chul. Journal of Korean Nuclear Society. Calculation of Neutron and Gamma-ray Flux-to-Dose-Rate Conversion Factors 1980;12(3).
[17] International Electrotechnical Commission, Protective devices against diagnostic medical X-radiation - Part 1: Determination of attenuation properties of materials, IEC 61331-1:2014.
[18] Currie Lloyd A. Analytical chemistry limits for qualitative detection and quantitative determination. Anal Chem 1968;40(3):586–93.
[19] BIPM, IEC, IFCC, ISO, IUPAC, IUPAP and OIML. Joint Committee for Guides in Metrology, Guide to the expression of uncertainty in measurement. (BIPM: Sèvres) 2008.
[20] Sharaf JM, Saleh H. Gamma-ray energy build up factor calculations and shielding effects of some Jordanian building structures. Radiat Phys Chem 2015;110:87–95.